Analysis of the Requirements for Tomographic SAR Acquisitions for 3-D Forest Structure Applications

Victor Cazcarra-Bes[a], Matteo Pardini[a], and Konstantinos Papathanassiou[a]
[a]German Aerospace Center (DLR),Microwaves and Radar Institute, Wessling, Germany.

Abstract

Synthetic Aperture Radar Tomography (TomoSAR) is the unique remote sensing technique able to extract 3-D information over forests at global scale, with continuous coverage and independently of cloud coverage. However, the usual low number of acquisitions in TomoSAR limits its imaging capability to extract 3-D forest information. In this paper, different number and distributions of acquisitions are analyzed in terms of vertical resolution and peak-sidelobe level (PSL). Simulations of TomoSAR data supported by point cloud lidar for realistic scenarios are discussed in terms of vertical profiles. The results show that, for a limited number of tracks, a non-uniform distribution with higher vertical resolution and PSL is necessary to characterize different forest structure types.

1 Introduction

3-D forest structure is a key indicator of the forest ecosystem and it is used for the estimation of many forest related products such as biomass, productivity or biodiversity [1]. The use of single-tree measurements on the ground allows a detailed description of the forest, but the effort to collect the data limits the spatial coverage and the temporal sampling. From the wide range of remote sensing techniques that allow large coverage and frequent revisit times, Synthetic Aperture Radar (SAR) Tomography (TomoSAR) provides the capability to get 3-D measurements at high-resolution with continuous and large area coverage independently of the weather or cloud coverage conditions [2].

TomoSAR combines several SAR images (over the same area) acquired along different acquisitions or orbits to obtain the backscattered power of the different forest elements in the height direction (i.e. vertical reflectivity profiles). Low frequencies (e.g. L-band) penetrate and interact with the canopy elements until the ground before coming back to the sensor. Due to these unique characteristics, TomoSAR is nowadays a technique to be potentially considered to measure 3-D structure properties of the forest [3]. Examples of this new trend are the upcoming SAR missions ESA BIOMASS [4] and Tandem-L [5], that will provide TomoSAR acquisitions worldwide.

Assuming a proper calibration of the SAR data [2], with low system errors and no temporal (or small) decorrelation between each SAR image, the quality of the vertical TomoSAR profiles is defined by the geometry of each acquisition (i.e the vertical wavenumber associated to each image pair [2]) and the total number of individual SAR acquisition used for the TomoSAR processing. In a realistic TomoSAR scenario, the number of SAR images is limited due to the cost, the flight/orbital and/or temporal constraints. Therefore, the design of a TomoSAR system in terms of number and distribution of acquisitions is a critical issue.

Different parameters characterize a TomoSAR system in order to extract 3-D forest structure information. The first one is the height of ambiguity, which is related to the minimum distance among acquisitions, and it is commonly fixed to a value higher than the maximum expected tree height in the forest. The second one is the vertical resolution, which is related to the maximum track separation among the acquisitions. A higher vertical resolution is always desired for a TomoSAR system in order to detect multiple forest layers, but if the number of images is limited, a higher vertical resolution implies a non-uniform distribution of the acquisitions. This is translated into a decrease of the performance of the Point Spread Function (PSF), which can lead to an ambiguity between the real canopy layers and the sidelobes from the system geometry.

For the performance analysis of the PSF, different parameters such as the peak-sidelobe level (PSL) or the integrated sidelobe ratio (ISLR) can be used. The PSL expresses the ratio between the returned signal first sidelobe respect the main lobe of the PSF, while the ISLR represents the sum of energy in the sidelobes, divided by the sum of energy in the mainlobe. For forest structure applications, where the local maxima of the TomoSAR profiles are interpreted as canopy forest layers to characterize the forest structure [6, 7], the PSL is a crucial parameter. Non-desired higher values of PSL can be wrongly interpreted as canopy layers in the resulting TomoSAR profiles, which can result in a wrong characterization of the forest structure [8]. Regarding the ISLR, although in general low values are desired, a high sidelobe with low energy will affect much more the interpretation of TomoSAR results than a sidelobe with more energy but spread over different heights. Therefore, the PSL together with the vertical resolution are considered the

main parameters to characterize the TomoSAR acquisition for forest structure applications.

In this context, the goal of this paper is to analyze the effect of different TomoSAR configuration scenarios (i.e. different vertical resolutions, PSL levels and number of acquisitions). First, to properly design a TomoSAR system, an optimization of the position of acquisitions based on the minimization of the PSL is done. Second, for a selected number of scenarios a simulation of the TomoSAR acquisition supported by a point cloud lidar of a temperate forest is performed. Finally, the results for realistic TomoSAR scenarios in terms of vertical reflectivity profiles over different forest structure areas are discussed.

2 Distribution of acquisitions

2.1 Uniform

A common strategy followed in TomoSAR is to use a uniform distribution of acquisitions, with a separation large enough to produce a safety height of ambiguity for the observed forest scenario. However, if the acquisitions are uniformly distributed, the only way to increase the vertical resolution is to increase the number of available acquisitions. This is not always possible due to the cost, flight/orbit constraints or large temporal separation between each acquisition, which leads to decorrelation effects. Figure 1 shows the PSL and the vertical resolution depending on the number of acquisitions used. As seen in Figure 1, for a completely uniform distribution the PSL is low enough to have a good performance already with four or five acquisitions. However, for this low number of acquisitions the vertical resolution is very poor (between 25 to 30 m). Therefore, to increase the vertical resolution is necessary to increase the number of acquisitions or to distribute them in a non-uniform way.

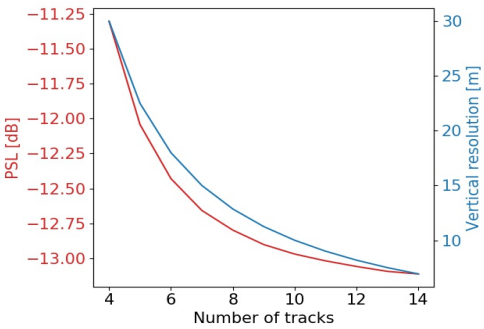

Figure 1 PSL (red) and Vertical resolution (blue) for a different number of uniformly distributed acquisitions with a fixed height of ambiguity of 85 m.

2.2 Non-uniform distribution with minimum PSL

As mentioned in section 2.1, non-uniform distributions of acquisitions must be used in order to increase the vertical resolution with a low number of acquisitions. However, the reduction on the number of acquisitions for a fixed vertical resolution, implies an increase of the PSL, which can cause problems in the interpretation of the TomoSAR results to extract forest structure information [8]. Therefore, a trade-off between vertical resolution and PSL level is needed to properly design a TomoSAR system.

2.2.1 *Free* distribution

In order to distribute the acquisitions, a minimization procedure of the PSL is used [9]. More in detail, given some constraints (such as the height of ambiguity or the vertical resolution) and the number of desired acquisitions, the minimization procedure looks for the distribution that minimizes the PSL. In other words, the acquisitions can be freely distributed in any position in order to minimize the PSL. The vertical resolution, the number of acquisitions and the height of ambiguity (always at 85 m.) are fixed and used as constraints for the minimization procedure.

Figure 2 shows the performance (in terms of PSL) obtained for different combinations of vertical resolution and number of acquisitions. Therefore, if the number of acquisitions is fixed (for example due to temporal or orbital constraints), Figure 2 can be used to have an idea of the achieved performance in case there are no more constraints (for example on the positions of the acquisitions). As an example of the interpretation of Figure 2, if the number of acquisitions is limited to 6, resolutions around 14 m provide low values (<-10 dB) of PSL. However, for higher vertical resolution the PSL increases to values around -6 dB for 6 m and -4 dB for 2 m of vertical resolution, respectively. From a different perspective, one can assume certain values of PSL and resolution as requirements in order to determine how many acquisitions are needed. For example, for -6 dB of PSL and 2 m of vertical resolution, a minimum 8 acquisitions are needed.

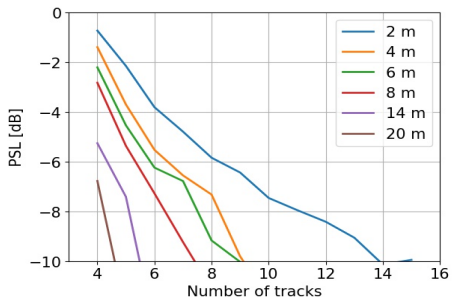

Figure 2 PSL for a *free* distribution strategy of the acquisitions for different vertical resolutions.

2.2.2 *Small* distribution

A different strategy to distribute the acquisitions is to fix not only the minimum vertical wavenumber (height of ambiguity) but also some acquisitions to *small* values of vertical wavenumber. Such a distribution allows to use the tomographic data set also for (model-based) forest height inversion [10]. The rest of the remaining vertical wavenumbers are freely distributed as in Section 2.2.1. For the simulations carried out in this paper four vertical wavenumbers to 0, 0.07, 0.14, 0.21 rad/m are fixed.

Figure 3 shows the PSL for the same fixed resolutions as in Figure 2. In this case, the minimum number of acquisitions

is six (as there are always four acquisitions in the fixed positions, plus one more to achieved the desired vertical resolution). The result show that, for the *small* distribution, the values of the vertical wavenumbers allow forest height inversion methodologies and the performance in terms of PSL is only slightly reduced with respect to the *free* distribution.

It is important to take into account that the position of the acquisitions are freely distributed in order to achieved the best possible PSL performance, but this freedom can be constraint in real scenarios due to orbit/flight constraints. This would lead to a worse performance as the ones obtained in sections 2.2.1 and 2.2.2 as it will reduce the potential available positions.

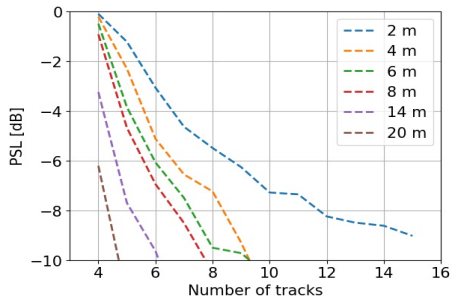

Figure 3 PSL for a *small* vertical wavenumbers distribution strategy for different vertical resolutions.

3 Simulation of the covariance

In order to evaluate the effect of tomographic configurations, different tomographic simulations are performed. For the simplest case of a point scatter at position x, y and the associate vertical wavenumber k_z for a give acquisition pair, the phase difference is given by:

$$\phi = e^{-ik_z h(x,y)}, \tag{1}$$

where $h(x, y)$ is the height of the scatter at position x, y. Assuming a set of n scatters $S(x, y, z)$ in the 3D space, the phase difference c for an acquisition pair can be obtained as the sum of the individual contributions of each scatter:

$$c = \sum_{i=1}^{n} e^{-ik_z S_n}, \tag{2}$$

Equation 2 provides the simulated spectral sample for the corresponding k_z difference between a pair of acquisition. Given M acquisitions with their corresponding k_z values, an MxM-dimensional covariance matrix R can be defined by accounting for the k_z difference between all acquisitions. Therefore, the matrix R represents the whole tomographic acquisition.

3.1 Tomographic inversion

The phase differences between each of the acquisitions define the so-called steering vector at a given height h_0:

$$a\left(z_0\right) = \left[1, e^{jk_{z1}z_0},\ e^{jk_{z2}z_0},\ \ldots, e^{jk_{zn}z_0}\right], \tag{3}$$

From the steering vector defined in 3, the steering matrix A is defined as:

$$A = a_z a_z^H, \tag{4}$$

where $()^H$ stands for the Hermitian or transpose conjugate operator. Then, with the covariance matrix R previously obtained and the steering matrix A, the tomographic inversion problem can be expressed as [2]:

$$R = Af, \tag{5}$$

where f represents the backscattered power along the heights (i.e. the reflectivity profile of the forest). Many algorithms can be used to reconstruct the 3-D radar reflectivity of the scene depending on different factors such as the use (or not) of a model, the desired type of output (e.g. less or more sparse result), the amount and quality of the SAR data (i.e number and distribution of acquisitions), etc. Therefore, the choice of one or another TomoSAR inversion method is not straightforward and will highly depend on the desired application and performance. In this paper, the Fourier Beamforming is selected as algorithm for the TomoSAR inversion. Fourier Beamforming is one of the most used algorithms for TomoSAR studies, it allows an easy and clear interpretation of the results without including any model or constraints in the estimation of the 3-D radar reflectivity. A more detailed explanation and comparison between different TomoSAR techniques can be found in [11, 12].

3.2 Lidar point clouds

Ir order to make a realistic simulation, real lidar point clouds are considered to define the scatters of the scene. The forest test site is located near the city of Traunstein, in Germany. It is a managed temperate forest that contains different structure types. The managed area of the forest covers around 25 ha, where all the trees (position, species and diameter) are measured. This detailed information allows differentiating the forest structure areas. Figure 4 shows the tree canopy height obtained by an airborne Lidar system in 2016 and the different forest structure areas delimited by colored polygons. The black polygon on the left part is characterized by a high heterogeneous structure with multi-species and tall trees. In the middle, the red polygon shows a *gap* in the forest with only a few scattered trees. Finally, in the right side, the orange and blue polygons define mono-species and homogeneous areas.

4 Results

A uniform Tomographic acquisition with 50 acquisitions is simulated to generate a reference case scenario. This scenario represents an *ideal* situation with many acquisitions that allows a perfect characterization of the scene. Figure 5 (a) shows the normalized reflectivity (also known as tomogram) over the white line in Figure 4. The high performance in terms of PSF and vertical resolution given by this scenario allows to distinguish the different scatters and areas of the forest. However, the tomographic result

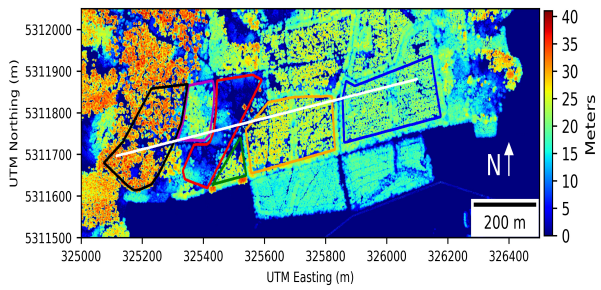

Figure 4 Lidar height over the forest test site in Traunstein, Germany. Each polygon represents a different forest structure type.

of Figure 5 (a) is an ideal case with too many acquisitions. In a more realistic scenario, constraints such as the orbit, the cost or the temporal separation between acquisitions can reduce the available data for a TomoSAR study. As a consequence, if less acquisitions are available the performance decreases respect to the one in Figure 5 (a) depending on how this acquisitions are distributed (i.e the vertical wavenumber k_z between them).

4.1 Uniform distribution

As mentioned in section 2.1, a uniform distribution is a usual way to acquired TomoSAR data. Figure 5 (b), (c), (d) show the Fourier Beamforming result over the white line in Figure 4 with a height of ambiguity of 80 m. and vertical resolutions of 6 m. (15 acquisitions), 9 m. (10 acquisitions) , and 21 m. (5 acquisitions), respectively. As expected from Figure 1, the use of a completely uniform distribution allows to obtain a really good performance in terms of PSL. This can be clearly seen in the higher contrast between the areas where the canopy is expected and the areas with no scatters. On the contrary, the use of a completely uniform distribution implies a reduction of the vertical resolution, which can be problematic when the number of tracks is low. This effect can be observed in Figure 5 (d) where in some areas (e.g. around sample 1100) the ground layer is not detected. The reduction of the number of acquisitions is also reflected in terms of root mean square error (RMSE) respect to the ideal case scenario. The RMSE increases from a value of 0.13 for the case of 15 acquisition until 0.17 and 0.3 for the case of 10 and 5 acquisitions, respectively.

4.2 Non-uniform distribution

Currently, all TomoSAR data sets are obtained by aircrafts with the possibility to acquired several SAR images (typically from 7 to 15 or even more) in a short revisit time. Although some investigation show the possibility to make SAR tomography with the existing satellites [13, 14, 15], there is not yet a SAR satellite mission that acquires TomoSAR data in a systematic way. In the near future, it is expected that the new space SAR missions (such as the ESA BIOMASS [4]) will provide TomoSAR data continuously. However, the amount of SAR images for the TomoSAR processing will be reduced (respect to the actual aircraft acquisitions) down to four or seven acquisition in the best case. In this section, a conservative scenario of five acquisitions is considered.

As mentioned in Section 4.1, for a dataset of five acquisitions with a uniform distribution (see Figure 5 (d)) the tomographic results lead to mix different layers in some areas of the forest due to the low vertical resolution achieved with only five images. As discussed in section 2.2, a way to increase the resolution with the same number of acquisitions is to redistribute the acquisitions in a non-uniform way. Figures 5 (e), (f) and (g) show the result for a freely distribution of each acquisition for 4 m., 8 m. and 12 m. of vertical resolution respectively. Although the minimization procedure to select the positions of each acquisition gives the lowest possible PSL, the tomograms in Figure 5 (e), (f) and (g) have a clear degradation in terms of PSL respect to the one in Figure 5 (d). This degradation of the PSL is also reflected in terms of RMSE from 0.41 in Figure 5 (e) until 0.29 and 0.27 for Figures 5 (f) and (g), respectively. However, this degradation of the PSL goes in favour of an increase of the resolution. Both effects can be clearly seen in the ground area (around sample 550), where the uniform distribution example has a wider ground and lower sidelobes compare to the examples with a free distribution.

4.3 Analysis of forest structure polygons

For a further analysis over the different forest structure areas, the distribution in Figure 5 (f) with a resolution of 8 m. is selected to be compared with the uniform distribution. The chose is a trade of between the good PSL performance obtained in Figure 5 (e) and the lower vertical resolution of Figure 5 (g). Figure 6 shows vertical profiles in each of the different forest structure polygons defined in Figure 4 for the two scenarios using only five acquisitions, as well as the ideal scenario generated with 50 uniformly spaced acquisitions.

The forest structure type of the black polygon shows a similar performance for both scenarios. This polygon is characterized by the highest trees in the whole forest with a non-dense amount of tree. These two characteristics allow a nice discrimination of the two layers present in the ideal case for both scenarios with a slightly better discrimination of te ground layer by the free distribution. The next polygon towards the east (purple in Figure 4) is characterized by an homogenous area, which leads to a small contribution of the ground (see blue line) that makes it almost not detectable by the uniform distribution (orang line). In the middle of the forest, there is the red polygon, which is mainly a ground area. The profiles over this polygon are a nice example of the low resolution for the uniform distribution (wide main lobe) and a worse PSL for the free distribution. Finally, for the last two polygons (orange and blue in Figure 4) the uniform distribution is not able to detect the ground layer, while the free distributed scenario can detect both layers. In this case, although there is a stronger contribution of the ground respect to the purple polygon, the lower tree heights respect to the black polygon makes the separation not possible for a vertical resolution 21 m given by the uniform distribution. Therefore, although the RMSE is similar for both (0.3 for the uniform and 0.29 for

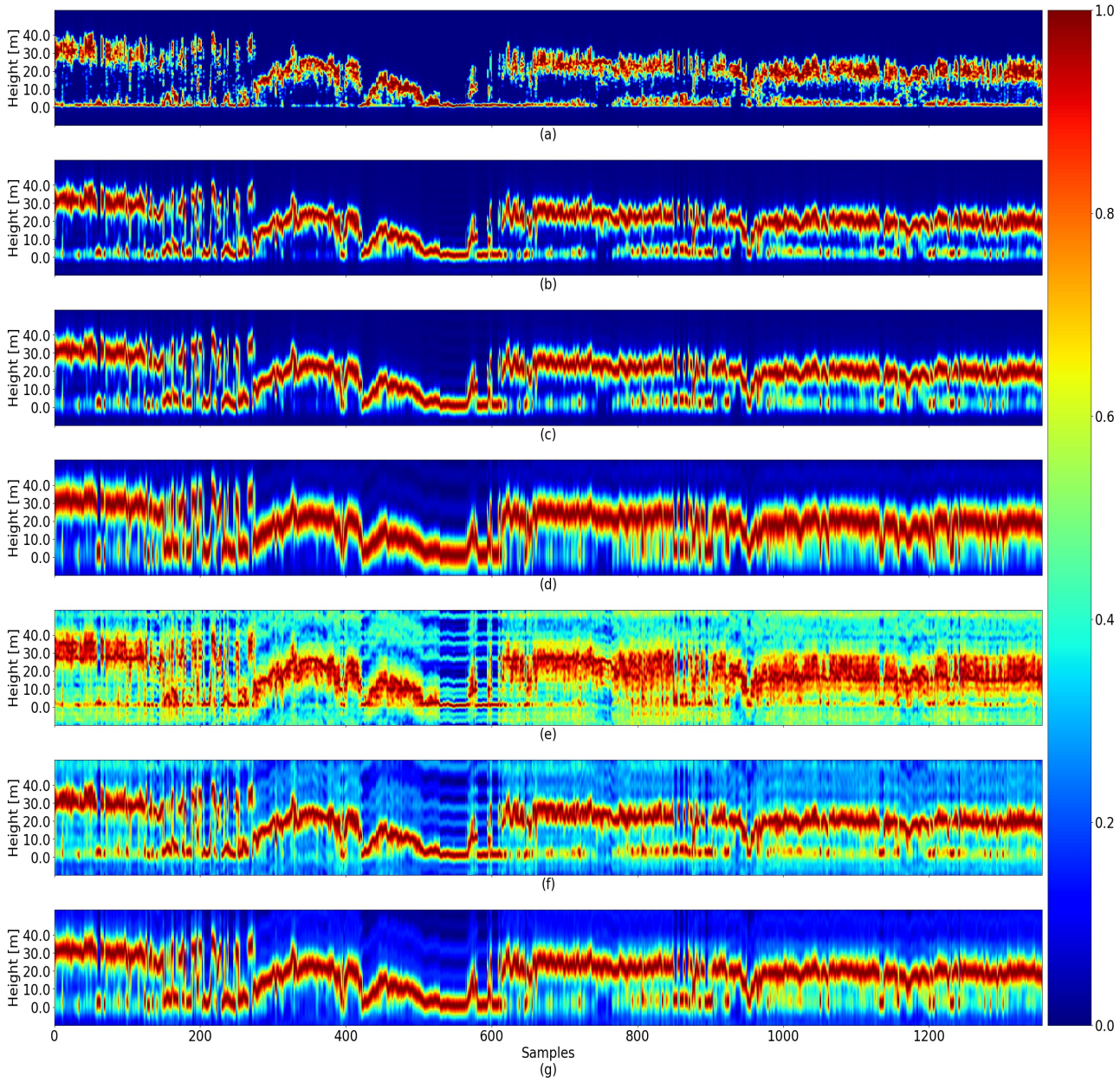

Figure 5 Fourier beamforming of the simulated coherence at the positions of the lidar point clouds. (a) 50 uniformly spaced acquisitions with 1 m of vertical resolution, (b) 15 uniformly spaced acquisitions with 6 m of vertical resolution, (c) 10 uniformly spaced acquisitions with 9 m of vertical resolution, (d) 5 uniformly spaced acquisitions with 21 m of vertical resolution, (e) 5 freely spaced acquisitions with 4 m of vertical resolution, (f) 5 freely spaced acquisitions with 8 m of vertical resolution and (g) 5 freely spaced acquisitions with 14 m of vertical resolution.

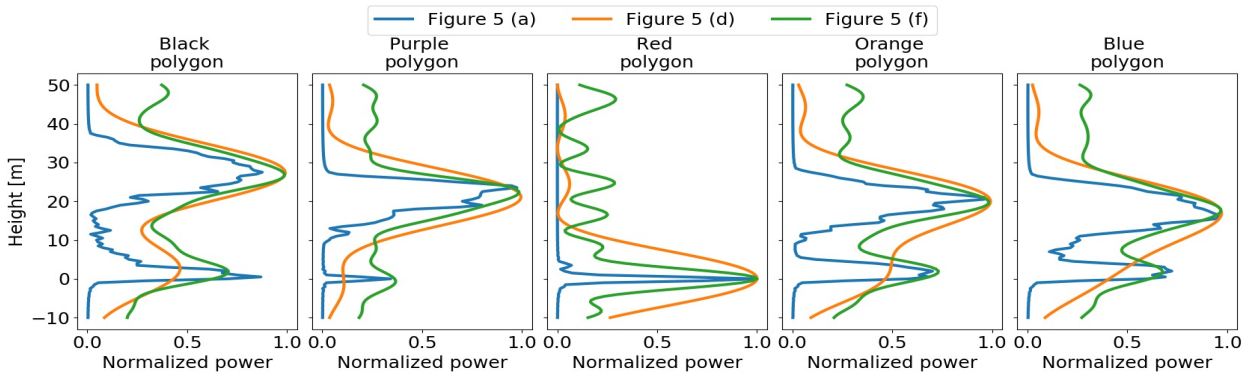

Figure 6 Vertical reflectivity profiles over the different forest structure polygons shown in Figure 4

the free distribution), the analysis of the profile in terms of detection of layers for different forest structure types, suggests that certain degradation of the PSL is preferred in order to achieve a better vertical resolution.

5 Conclusions

In this paper, an analysis of the requirements for a TomoSAR acquisition is done. The trade-offs in the design in terms of peak sidelobe level (PSL), number of acquisitions and resolution have been discussed taking into account different strategies to distribute the acquisitions on a TomoSAR system. First, a uniform distribution has been considered as the standard approach. Then, the acquisitions have been freely distribute in order to achieved the lowest possible PSL. Additional constraints, such as fixed lower values of k_z have been used in order to account not only for the estimation of the vertical reflectivity profile, but also for further applications like forest height that require lower values of k_z. Simulation of distributed point scatters have been used to evaluate different TomoSAR scenarios. In order to make a realist simulation, lidar point clouds have been used to determine the positions of the scatters in the forest. The results show that, in general, if a large number of acquisitions (e.g. 10) are available, a uniform distribution is a good strategy. It provides a nice performance of the PSL and enough resolution with a controlled and expected result to extract 3-D forest information. However, if the number of acquisitions is limited (as in the case of future SAR missions) a uniform distribution strategy does not provide enough vertical resolution to completely characterize the forest. Therefore, a free distribution is necessary in order to increase the vertical resolution at the cost of having a worse PSL performance.

6 References

[1] R. Fischer, N. Knapp, F. Bohn, H. H. Shugart, and A. Huth, "The relevance of forest structure for biomass and productivity in temperate forests: New perspectives for remote sensing," *Surveys in Geophysics*, pp. 1–26, 2019.

[2] A. Reigber and A. Moreira, "First demonstration of airborne sar tomography using multibaseline l-band data," *IEEE Transactions on Geoscience and Remote Sensing*, vol. 38, no. 5, pp. 2142–2152, 2000.

[3] H. Aghababaee, G. Ferraioli, L. Ferro-Famil, Y. Huang, M. M. d'Alessandro, V. Pascazio, G. Schirinzi, and S. Tebaldini, "Forest sar tomography: Principles and applications," *IEEE geoscience and remote sensing magazine*, 2020.

[4] S. Quegan, T. Le Toan, J. Chave, J. Dall, J.-F. Exbrayat, D. H. T. Minh, M. Lomas, M. M. D'Alessandro, P. Paillou, K. Papathanassiou, *et al.*, "The european space agency biomass mission: Measuring forest above-ground biomass from space," *Remote Sensing of Environment*, vol. 227, pp. 44–60, 2019.

[5] A. Moreira, G. Krieger, I. Hajnsek, K. Papathanassiou, M. Younis, P. Lopez-Dekker, S. Huber, M. Villano, M. Pardini, M. Eineder, *et al.*, "Tandem-l: A highly innovative bistatic sar mission for global observation of dynamic processes on the earth's surface," *IEEE Geoscience and Remote Sensing Magazine*, vol. 3, no. 2, pp. 8–23, 2015.

[6] V. Cazcarra-Bes, M. Tello-Alonso, R. Fischer, M. Heym, and K. Papathanassiou, "Monitoring of forest structure dynamics by means of l-band sar tomography," *Remote Sensing*, vol. 9, no. 12, 2017.

[7] M. Tello, V. Cazcarra-Bes, M. Pardini, and K. Papathanassiou, "Forest structure characterization from sar tomography at l-band," *IEEE Journal of Selected Topics in Applied Earth Observations and Remote Sensing*, no. 99, pp. 1–13, 2018.

[8] V. Cazcarra-Bes, M. Pardini, and K. Papathanassiou, "Definition of tomographic sar configurations for forest structure applications at l-band," *IEEE Geoscience and Remote Sensing Letters*, pp. 1–5, 2020.

[9] R. Storn and K. Price, "Differential evolution–a simple and efficient heuristic for global optimization over continuous spaces," *Journal of global optimization*, vol. 11, no. 4, pp. 341–359, 1997.

[10] F. Kugler, S. Lee, I. Hajnsek, and K. P. Papathanassiou, "Forest height estimation by means of pol-insar data inversion: The role of the vertical wavenumber," *IEEE Transactions on Geoscience and Remote Sensing*, vol. 53, pp. 5294–5311, Oct 2015.

[11] V. Cazcarra-Bes, M. Pardini, M. Tello, and K. P. Papathanassiou, "Comparison of tomographic sar reflectivity reconstruction algorithms for forest applications at l-band," *IEEE Transactions on Geoscience and Remote Sensing*, vol. 58, no. 1, pp. 147–164, 2019.

[12] O. Frey and E. Meier, "Analyzing tomographic sar data of a forest with respect to frequency, polarization, and focusing technique," *IEEE transactions on geoscience and remote sensing*, vol. 49, no. 10, pp. 3648–3659, 2011.

[13] N. Ge, F. R. Gonzalez, Y. Wang, Y. Shi, and X. X. Zhu, "Spaceborne staring spotlight sar tomography—a first demonstration with terrasar-x," *IEEE Journal of Selected Topics in Applied Earth Observations and Remote Sensing*, vol. 11, no. 10, pp. 3743–3756, 2018.

[14] M. Pardini, A. Toraño-Caicoya, F. Kugler, and K. Papathanassiou, "Estimating and understanding vertical structure of forests from multibaseline tandem-x pol-insar data," in *2013 IEEE International Geoscience and Remote Sensing Symposium-IGARSS*, pp. 4344–4347, IEEE, 2013.

[15] M. Nannini, M. Martone, P. Rizzoli, P. Prats-Iraola, M. Rodriguez-Cassola, A. Reigber, and A. Moreira, "Coherence-based sar tomography for spaceborne applications," *Remote Sensing of Environment*, vol. 225, pp. 107–114, 2019.